COMPARISON BETWEEN THE PARABOLIC AND ELLIPTIC MODELS IN THE PULTRUSION PROCESS SIMULATION

Aluisio Viais Pantaleão – aluisio@mec.ita.cta.br
Cláudia Regina de Andrade - claudia@mec.ita.cta.br
Edson Luiz Zaparoli - zaparoli@mec.ita.cta.br
Instituto Tecnológico de Aeronáutica – Departamento de Energia – IEME
Pça Marechal Eduardo Gomes, 50 – Vila das Acácias – 12228-900 – São José dos Campos – SP - Brasil

Abstract. *Pultrusion is one of the most rapid and cost-effective processes for manufacturing composite materials with a constant cross-section. A fiber creel is impregnated in a resin bath and passes through a heated die with a constant pulling force. The elevated die temperature induces the curing resin process. The process is mathematically modeled by two equations: an elliptic energy equation and a transport equation for the degree of cure. These equations are coupled by a term-source resulting from resin curing exothermic reaction. A parabolic model, much simpler to be computationally implemented, can be used depending on the Péclét number of the problem. In this work the pultrusion process of thermosetting composite with circular cross-section is numerically simulated using an elliptic and a parabolic model. In both cases, the solution of the algebraic equations systems is obtained iteratively by a coupled way (no-segregated) combining the Conjugated Gradient and Newton-Raphson methods. The numeric data obtained for the temperature and degree of cure profiles through the two models were compared in order to verify the validity of the parabolic approach, that requests smaller computational effort. The temperature and the degree of cure distribution inside the pultruded material were also compared with results of the literature and showed a good agreement. It was analyzed the influence of the pulling speed and the fiber volume fraction on the results obtained by the elliptic and parabolic models.*

Key words: *Pultrusion, Composite Material, Carbon Fiber, Epoxy Resin, Degree of Cure.*

1. INTRODUÇÃO

Composite materials have a large industrial application (space and aeronautical structures, automotive components, tennis rackets). Pultrusion is one of the most rapid and cost-effective processes for manufacturing composite materials with a constant cross-section. In this process, a fiber creel is impregnated in a resin bath and passes through a heated die with a constant pulling force as represented in Fig. 1. The pulling speed, the fiber volume fraction, the die wall temperature profile, the type and quality of the fibers and resins, the composite thermal properties, are important parameters that affect the quality and performance of the manufactured material. Then, the improper control of these conditions

may result in a failure of the pultrusion process committing the mechanical properties of the final product (Kim et al, 1997).

Several authors have investigated the pultrusion process using mathematical models as well as experimental tests. The numerical study of Gorthala et al. (1994) presented a model solved by the finite difference technique to determine the temperature and degree of cure of the pultruded material.

Chachad et al. (1996) simulated the pultrusion process in transient regime applying the finite volume method. The authors analyzed the pultruded composite material characteristics with irregular cross-section.

Roux et al. (1998) presented numeric results and experimental measurements for the temperature profiles and degree of cure during the pultrusion process. The numerical solution was also obtained by the finite volume technique.

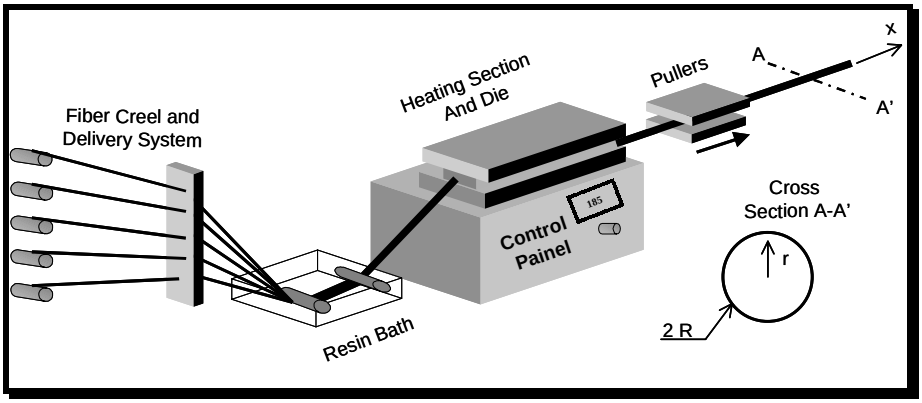

Figure 1. Schematic representation of the pultrusion process

In the work of Suratno et al. (1998), it was performed a numeric simulation of carbon fibers reinforced with resin epoxy, using the finite element method. The authors showed the effect of the pulling speed in the temperature and degree of cure axial profiles inside the composite material.

By comparing the results obtained using an elliptic and a parabolic model, the present study analyzes the pultrusion process of thermosetting composite with circular cross-section. The elliptic model equations were solved using the finite element technique with a Taylor-Galerkin scheme. The parabolic approximation equations were discretized in the cross-section of the pultruded bar by the Galerkin finite element and the axial direction (pulling axis) was evaluated by a time-like marching technique. Both models algebraic equations systems are solved iteratively by a coupled way (no-segregated) combining the Conjugated Gradient and Newton-Raphson methods. The effect of the pulling speed and the fiber volume fraction on the results obtained by the elliptic and a parabolic model is also investigated. The knowledge of these characteristics allows a better pultrusion process design.

2. MATHEMATICAL FORMULATION

The mathematical formulation is based in the following assumptions:

- the process is steady state and two-dimensional;
- the material properties (density, specific heat, thermal conductivity) are constant at any resin-degree of cure;
- the composite material is isotropic;
- the effect of pressure on the heat of reaction is neglected.

The present pultrusion process modeling is divided in two parts: the heat transfer problem and the resin-curing model. The heat transfer process that occurs within the pultruded composite is expressed as:

$$u\frac{\partial T}{\partial x} - \left(\frac{k_b}{\rho_b Cp_b}\right)\left[\frac{1}{r}\frac{\partial}{\partial r}\left(r\frac{\partial T}{\partial r}\right) + \frac{\partial^2 T}{\partial x^2}\right] = \dot{q} \tag{1}$$

with the boundary conditions:

at $x = 0$ (die entry) $\Rightarrow T = Te$ (1a)

at $r = R$ (bar/die interface) $\Rightarrow T = Tw(x)$ (1b)

where:

r – radial coordinate;

x – axial coordinate;

u – pull speed;

T – absolute temperature;

$\dot{q}$ – volumetric heat rate due to the resin-cure reaction;

ρ – density.

cp – specific heat

k – thermal conductivity

The bulk composite material density (ρ_b) is calculated by a mass fraction method given by:

$$\rho_b = \frac{1}{\frac{M_f}{\rho_f} + \frac{M_r}{\rho_r}}, \quad \text{and} \quad M_f = \frac{FV}{FV + \left(\frac{\rho_r}{\rho_f}(1 - FV)\right)} \tag{2}$$

where M is the mass fraction and the subscripts f, r and b correspond to fibers, resin and bulk composite material respectively. The thermal conductivity and the specific heat are determined in the same way:

$$k_b = \frac{1}{\frac{M_f}{k_f} + \frac{M_r}{k_r}} \quad \text{and} \tag{3}$$

$$Cp_b = FV\,Cp_f + (1 - FV)\,Cp_r \tag{4}$$

where FV is fiber volume fraction.

The degree of cure (α) is defined as the ratio between the energy liberated by the reaction until an instant of time (t) and the total energy liberated in whole cure reaction. The degree of cure variation with the time is calculated by:

$$\frac{D\alpha}{Dt} = \left[A\,exp\left(\frac{E}{RT}\right)\right](1 - \alpha)^n \tag{5}$$

where:

A – pre-exponential constant;

E – activation energy;

R – universal gas constant;
n – order of the reaction and
$\frac{D(\ )}{Dt} = u\frac{\partial(\ )}{\partial x}$ = steady state one dimensional substantial derivative.

The volumetric heat rate due to the resin-cure reaction is related to the degree of cure by the expression:

$$\dot{q} = \rho_r \left(1 - FV\right) \Delta H \frac{D\alpha}{Dt} \tag{6}$$

where:

ΔH – total heat of reaction per unit mass of resin.

The values of the constants in the Eqs. (5) and (6) are found from the data measured with differential scanning calorimeter (*DSC*). These parameters are provided by Suratno et al. (1998) and are listed in Table 1 for epoxy resin considered in this study.

Table 1. Kinetic parameter of epoxy resin

Parameter	Symbol	Value
pre-exponential constant	A	$1.914 \cdot 10^5$ (s^{-1})
activation energy	E	$6.05 \cdot 10^4$ (J mol^{-1})
total heat reaction	ΔH	$3.237 \cdot 10^2$ (J g^{-1})
order of reaction	*n*	1.69

Table 2. Carbon fiber and epoxy resin properties values

Properties	Carbon fiber	Epoxy resin
ρ (kg/m^3)	1790	1260
k (w/m·K)	11.6	0.2
Cp (J/kg·K)	712	1255

At the present work the epoxy resin is reinforced with carbon fibers and the required numerical values of the transport properties are shown in Table 2.

3. SOLUTION METHODOLOGY

The pultrusion process shown in Fig. 1 was modeled by Eqs. (1) to (6) that were solved by two different methodologies. In the former, named elliptic approach, the finite element technique with a Taylor-Galerkin scheme was implemented as described below:

3.1 Elliptic model: Taylor-Galerkin method

A general formulation that is similar to the energy equation of the convective heat transfer problem for Eqs. (1) and (5) is described by:

$$\frac{\partial \phi}{\partial t} + u\frac{\partial \phi}{\partial x} = \Gamma\left[\frac{1}{r}\frac{\partial}{\partial r}\left(r\frac{\partial \phi}{\partial r}\right) + \frac{\partial^2 \phi}{\partial x^2}\right] + G \tag{7}$$

with $\Gamma = \left(\frac{k_b}{\rho_b C p_b} \right)$ in Eq. (1) and $\Gamma = 0$ in Eq. (5).

When the Galerkin finite element method is applied to solve Eq. (7) it yields a physically reasonable solution only when the local mesh Péclét number (*Pe*) is less than 2. The *Pe* number is calculated by:

$$Pe = \frac{\rho_b \, u \, h}{\Gamma} \tag{8}$$

where *h* = finite element characteristic length scale along the pulling axis.

For large *Pe* number (problem dominated by convective transport) false oscillations appear in the solution process (Patankar,1980). To eliminate these spurious oscillations, Eq. (1) and Eq. (5) were solved using the Taylor-Galerkin finite element scheme (Donea, 1984 and Comini et al., 1995).

In this method the operator is split in two different contributions. At the first half of the pseudo-time integration interval only the convective terms are considered. The diffusive and source terms are carried on at the second half one. Thus, Eq. (7) is separated as:

$$\phi' = \frac{\partial \phi}{\partial t} = - u \, \frac{\partial \phi}{\partial x} \tag{9}$$

$$\phi' = \frac{\partial \phi}{\partial t} = \Gamma \left[\frac{1}{r} \frac{\partial}{\partial r} \left(r \frac{\partial \phi}{\partial r} \right) + \frac{\partial^2 \phi}{\partial x^2} \right] + G \tag{10}$$

For the first half of the time integration the time variation is calculated by a second-order Taylor series expansion:

$$\phi^{n+1/2} - \phi^n = \phi' \Delta t + \phi'' \frac{\Delta t^2}{2} + ... \tag{11}$$

where Δt = half of the pseudo-time integration interval.

The ϕ'' value in Eq. (11) is obtained time deriving Eq. (9):

$$\phi'' = \frac{\partial}{\partial t} [\phi'] = \frac{\partial}{\partial t} \left[- u \, \frac{\partial \phi}{\partial x} \right] = -u \frac{\partial \phi'}{\partial x} = -u \frac{\partial}{\partial x} \left[- u \, \frac{\partial \phi}{\partial x} \right] = u^2 \, \frac{\partial^2 \phi}{\partial x^2} \tag{12}$$

Combining Eq. (9), Eq. (11) and Eq. (12) results that:

$$\phi^{n+1/2} - \phi^n \approx \left[- u \, \frac{\partial \phi}{\partial x} \right] \Delta t + \left[u^2 \, \frac{\partial^2 \phi}{\partial x^2} \right] \frac{\Delta t^2}{2} \tag{13}$$

For the second half of the time integration the time variation is determined by a first-order Taylor series expansion, given by:

$$\phi^{n+1} - \phi^{n+1/2} = \phi' \Delta t + ... \tag{14}$$

Introducing the first time derivative of the Eq. (10) in Eq. (14), follows:

$$\phi^{n+1} - \phi^{n+1/2} \approx \left\{ \Gamma \left[\frac{1}{r} \frac{\partial}{\partial r} \left(r \frac{\partial \phi}{\partial r} \right) + \frac{\partial^2 \phi}{\partial x^2} \right] + G \right\} \Delta t \tag{15}$$

For the pseudo-transient scheme used in this work, Eq. (13) is added to Eq. (15) obtaining the equation used in the Taylor-Galerkin method

$$\phi^{n+1} - \phi^{n} \approx \left\{ - u \frac{\partial \phi}{\partial x} + \Gamma \left[\frac{1}{r} \frac{\partial}{\partial r} \left(r \frac{\partial \phi}{\partial r} \right) + \frac{\partial^2 \phi}{\partial x^2} + \left(\frac{u^2}{\Gamma} \frac{\Delta t}{2} \right) \frac{\partial^2 \phi}{\partial x^2} \right] + G \right\} \Delta t \tag{16}$$

The Taylor-Galerkin scheme inserts an artificial axial diffusion effect represented by the term below, which reduces the dependent variables axial gradients:

$$\left(\frac{u^2}{\Gamma} \frac{\Delta t}{2} \right) \frac{\partial^2 \phi}{\partial x^2} . \tag{17}$$

An unstructured mesh with triangular elements of six nodes and second-degree interpolation polynomials was applied to Eq. (16). The resultant algebraic equations system was solved by an iterative procedure in a coupled (no-segregated) way combining the Conjugated Gradient and Newton-Raphson methods. An adaptive scheme was used with successive mesh refinement in the more intense gradient regions. Fig. 2 presents an intermediate computational grid in the solution process for the elliptic formulation:

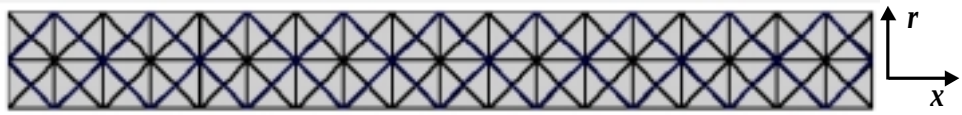

Figure 2. Computational grid in the intermediate process solution.

3.2 Parabolic model: a time-like marching method

In the parabolic model the Eq. (1) is simplified by neglecting the axial conduction term, as follow:

$$u \frac{\partial T}{\partial x} - \left(\frac{k_b}{\rho_b C p_b} \right) \left[\frac{1}{r} \frac{\partial}{\partial r} \left(r \frac{\partial T}{\partial r} \right) \right] = \dot{q} \tag{18}$$

In this approximation Eq. (5) and Eq. (17) were discretized in the pultruded bar cross-section by the Galerkin finite element and the axial direction (pulling axis) was evaluated by a time-like marching technique.

The solution was obtained using a scheme equivalent to Crank-Nicolson time differencing. The cubic term in the Taylor series expansion of the solution in time is determined by a three-step approach. The time-step is controlled so this cubic term is less than an imposed error limit.

Fig. 3 resents an intermediate computational grid in the solution process for the parabolic formulation. The computational domain is represented by a circular sector of the entire duct cross-section due to circular invariance.

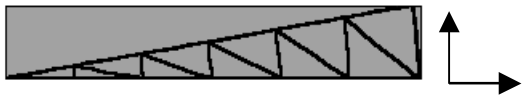

Figure 3. Computational grid in the intermediate process solution.

4. RESULTS

A comparison between the elliptic Taylor-Galerkin (T-G) and the parabolic results for the pultrusion process is presented in Fig. 4. The Taylor-Galerkin formulation was simulated for different Δt values. For $\Delta t = 1.10^{-1}$ the axial diffusion influence is negligible for and the results approximate the parabolic method ones. The axial temperature and the degree of cure distributions show that the artificial axial diffusion effect in the Taylor-Galerkin method results increases for higher Δt values. For $\Delta t = 1$, there is a good agreement between the elliptic and parabolic results and the stability of the Taylor-Galerkin scheme is higher. So, all the following results were obtained with $\Delta t = 1$ and the parameter listed previously in Tables 1 and 2.

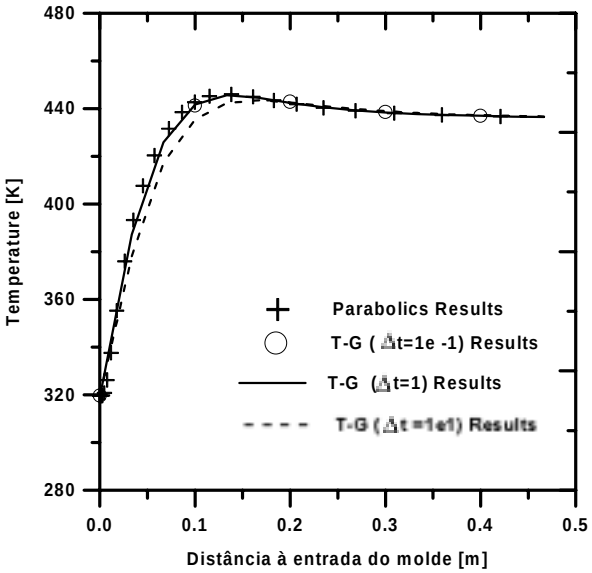

Figure 4a. Elliptic and parabolic results for the axial temperature profile (u = 0,1/60 m·s^{-1} and FV = 0,7)

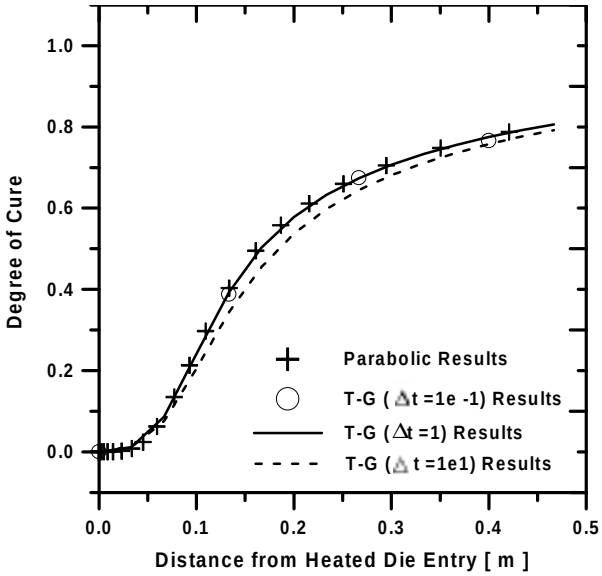

Figure 4b**.** Elliptic and parabolic results for the axial degree of cure profile (u = 0,1/60 m·s^{-1} and FV = 0,7)

The numerical results using the Taylor-Galerkin scheme and the parabolic approximation were also compared with the data presented in Suratno et al. (1998). The axial temperature and the degree of cure profiles are showed in Fig. 5. The simulations were carried out with the same wall temperature distribution provided in Suratno's work (dashed curve in Fig. 5a). Both temperature and degree of cure distributions obtained by the elliptic and parabolic schemes don't differ significantly from the Suratno's data.

The temperature profile exhibits a maximum value close to the mid-die extension (Fig. 5a) due to the heat released by the resin cure exothermic reaction. It is noticed that in the region near the die entry the degree of cure shown in Fig. 5b present small variation, but the curve elevates rapidly as the resin cure reaction begin, reaching almost 90% in the die exit.

This abrupt increase is associated with the temperature elevation in the composite material that also is influenced by the degree of the cure evolution, showing that these two phenomena are coupled.

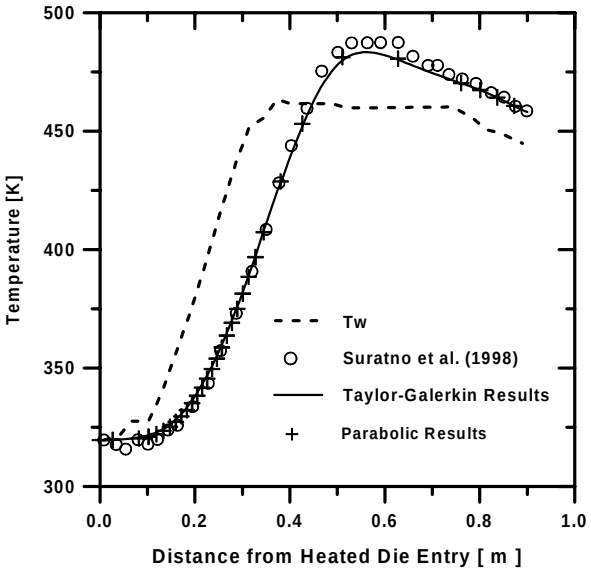

Figure 5a. Results for the axial temperature profile (u = 0,1/60 m·s^{-1}and FV = 0,7)

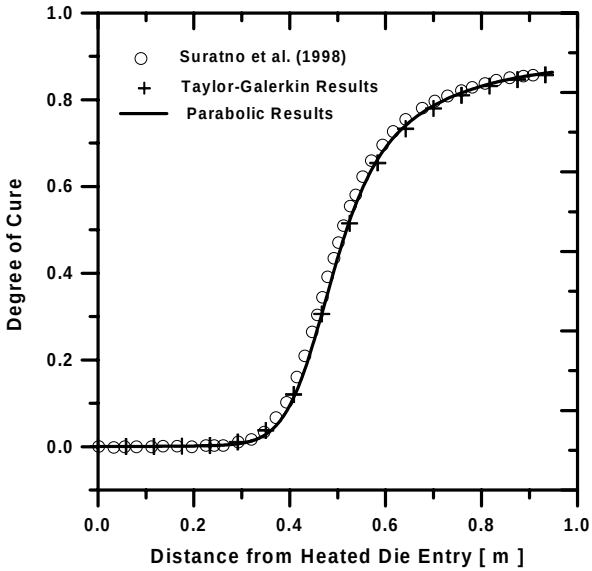

Figure 5b. Results for the axial degree of cure profile (u = 0,1/60 m·s^{-1} and FV = 0,7)

The influence of the pulling speed in the pultrusion process is presented in Fig. 6. The maximum value in the axial temperature distribution (Fig. 6a) occurs at smaller distance the die entry die when the pulling speed is small. Curves with higher values of the pulling speed exhibit a retarded and smoothed temperature peak. This displacement in the temperature maximum value is associated with a delay in the evolution of the degree of cure shown in Fig. 6b. It is also verified that the Taylor-Galerkin and parabolic distributions present a good agreement (Figs. 6a and 6b) and both results show that higher pulling speed values require a greater die extension to complete the cure process.

Table 3. Comparison between Taylor-Galerkin and parabolic schemes (Degree of Cure = 0,98, u = 0,1/60 m·s^{-1}and FV = 0,7)

Error	CPU Time (hours)	
	T. Galerkin	Parabolic
1.10^{-3}	00:28:18	00:00:05
1.10^{-4}	00:41:50	00:00:09
1.10^{-5}	11:21:03	00:00:22

Table 3 presents the computational time processing for Taylor-Galerkin and parabolic schemes as a function of the imposed numeric solution accuracy (error). It is verified that the

parabolic approximation requires much smaller computational time processing in comparison with the elliptic model.

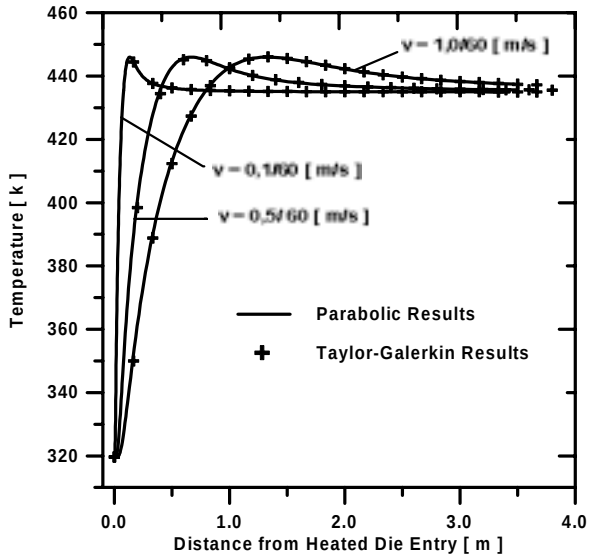

Figure. 6a – Axial temperature profile along the die extension for different pulling speed values and *FV = 0.7*

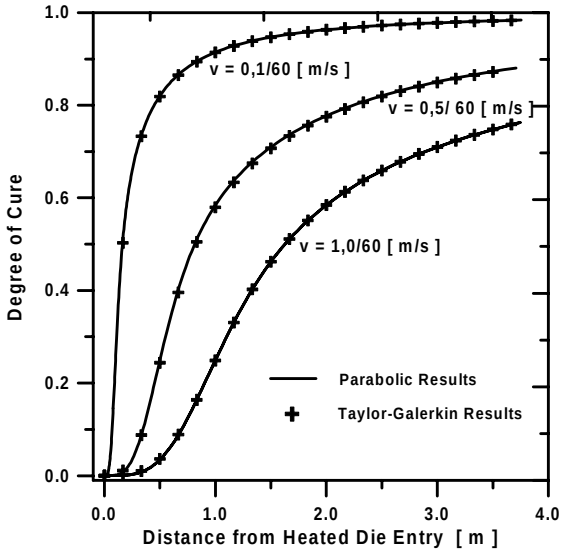

Figure. 6b – Axial degree of cure profile along the die extension for different pulling speed values and *FV = 0.7*

Fig. 7 presents the effect of the fiber volume fraction in the temperature and degree of cure distributions during the manufacture process of epoxy resin reinforced with carbon fibers. The temperature curve (Fig. 7a) shows that for *FV = 0.4* the resin cure reaction is more abrupt resulting in a high temperature elevation close to the die entry. As the fiber to resin ratio increases, this maximum temperature value decreases but the final temperature value is quite the same one for the three *FV* values simulated. The axial degree of cure as a function of the fiber volume fraction is presented in Fig. 7b.

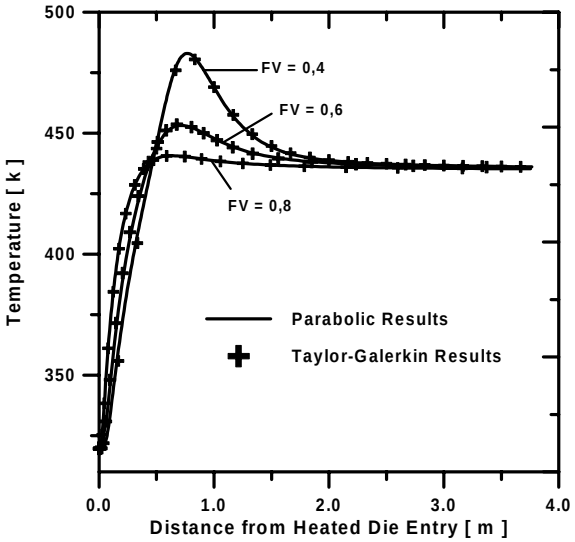

Figure. 7a – Axial temperature profile along the die extension for different fiber volume fraction values and u = 0,5/60 m·s^{-1}

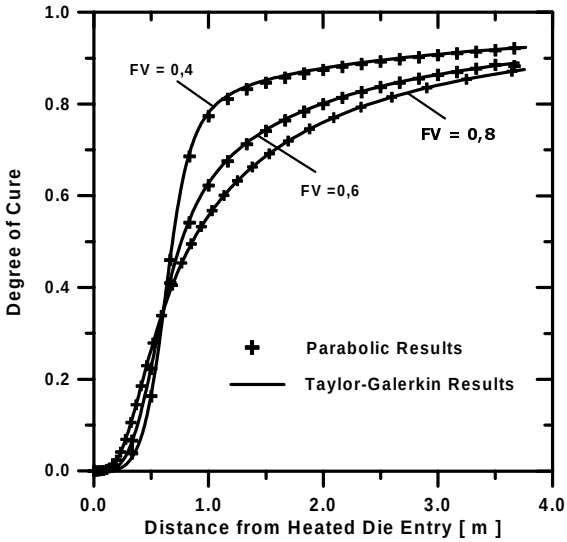

Figure. 7b – Axial degree of cure profile along the die extension for different fiber volume fraction values and u = 0,5/60 m·s^{-1}

At the die entry (when the cure reaction didn't still don't started) the curve for *FV = 0.8* exhibits a degree of cure slightly greater. As soon as the exothermic reaction beginS, the degree of cure distribution with *FV = 0.4* elevates abruptly while the curves for *FV = 0.6* e *FV = 0.8* present a smoother increase.

At the die exit, both elliptic and parabolic methods results for axial degree of cure profile is higher when *FV = 0.4* (Fig. 7b). However, as noted by Kim et al (1997), the manufacture of pultruded bars with small fiber to resin composition ratio can commit the mechanical resistance of the final composite material.

5. CONCLUSIONS

At this work the pultrusion process was numerically simulated using the finite element method. A comparison between an elliptic model (Taylor-Galerkin) and a parabolic approximation showed a good agreement for the axial temperature and degree of cure distributions for small pseudo time stop integration. Although, it is important to note that the parabolic scheme has some advantages: it requires smaller computational time processing and is easier to be implemented than the elliptic model.

The results also showed that the pulling speed and the fiber volume fraction are important parameters that affect the degree of cure and the final product quality.

Both methodologies were shown appropriate to analyze the heating system characteristics, allowing a better equipment project and could be applied in other fiber/resin composite materials.

6. ACKNOWLEDGES

The authors are grateful to FAPESP (grant #99/03471-5) and CNPq (grant #146405/ 1999-4) by the support to development of this work.

7. REFERÊNCIAS BIBLIOGRÁFICAS

Chachad, Y. R., Roux, J.A., Vaughan, J.G. e Arafat, E. S., 1996,*"Thermal Model for Three - Dimensional Irregular Shaped Pultruded Fiberglass Composities"*, Journal of Composities Materials, 30(6): 692-721.

Comini, G., Manzan, M. e Nonino, C., 1995, "Analysis of Finite Element Schemes for Convective-Type Problems ", International Journal for Numerical Methods in Fuids, 20: 443-458.

Donea, J., 1984, "A Taylor-Galerkin Method for Convective Transport Problems", International Journal for Numerical Methods in Engineering, 20: 101-119.

Gorthala, R., Roux, J.A. e Vaughan, J.G., 1994, "Resin Flow, Cure and Heat Transfer Analysis for Pultrusion Process", Journal of Composities Materials, 28(6): 486-506.

Kim, D. W., Han, P. G., Jin, G. H. e Lee, W. I., 1997, "A Model for Thermosetting Composite Pultrusion Process", Journal of Composities Materials, 31: 2105-2122.

Patankar,S.V., 1980, "Numerical Heat Transfer and Fluid Flow", Hemisphere Publishing Corporation, Washington.

Suratno, R. B., Ye, L. e Mai, Y. W., 1998, "Simulation of Temperature and Curing Profiles in Pultruded Composities Rods", Composities Science and Technology, 58: 191-197.

Roux, J.A, Vaughan, J.G., Shanku, R., Arafat, E. S., Bruce, J. L. e Johnson, V. R.,1998," Comparison of Measurement and Modeling for Pultrusion of a Fiberglass-Epoxy I-Beam", Journal of Reinforced Plastics and Composities, 17: 1557-1579.